

# physica **p** status **s** solidi **S**

[www.pss-journals.com](http://www.pss-journals.com)

**reprint**



# Spontaneous spin polarization and spin pumping effect on edges of graphene antidot lattices

K. Tada<sup>1</sup>, T. Hashimoto<sup>1</sup>, J. Haruyama<sup>\*1</sup>, H. Yang<sup>2</sup>, and M. Chshiev<sup>2</sup>

<sup>1</sup>Faculty of Science and Engineering, Aoyama Gakuin University, 5-10-1 Fuchinobe, Sagami-hara, Kanagawa 252-5258, Japan

<sup>2</sup>SPINTEC, CEA/CNRS/UJF-Grenoble 1/Grenoble-INP, 38054 Grenoble cedex 9, France

Received 6 April 2012, revised 14 June 2012, accepted 10 September 2012

Published online 23 October 2012

**Keywords** antidot lattices, graphene, nanopores, spin polarization, spin pumping

\* Corresponding author: e-mail j-haru@ee.aoyama.ac.jp, Phone/Fax: +81-42759-6256

The zigzag-type atomic structure at edges of graphenes theoretically produces flat energy band. Because electrons have infinite effective mass at the flat band, they localize at zigzag edges with high densities. The localized electron spins are spontaneously polarized due to mutual Coulomb interaction in spite of a material consisting of only carbon atom with  $sp^2$  bonds. However, in most experimental studies, spin polarization (such as ferromagnetism) has been observed in defect-related carbon systems. Here, we fabricate honeycomb-like arrays of low-defect hexagonal antidots (nanopores)

terminated by hydrogen atoms on graphenes. They are prepared by a non-lithographic method using nanoporous alumina templates. We find large-magnitude ferromagnetism arising from polarized electron spins localizing at the zigzag antidot edges. Moreover, weak hysteresis loop in magnetoresistance and also spin pumping effect are found for perpendicular and parallel magnetic fields applied to the few-layer antidot lattices with larger inter-antidot space. These promise to be a realization of rare-element free magnets and also novel spintronic devices such as all-carbon spin transistors.

© 2012 WILEY-VCH Verlag GmbH & Co. KGaA, Weinheim

**1 Introduction** Many theories have predicted the appearance of spin polarization (e.g., ferromagnetism) in carbon-based  $sp^x$ -orbital systems from the viewpoints of edge-localized electrons [1–8]. In particular, zigzag-edge atomic structures of graphene (Fig. 1a) have been of great interest [1–6, 9–25].

Assuming perfect edges without defects, the electron spins localizing at zigzag edges [1, 9] are stabilized and spontaneously polarized due to the exchange interaction between the two edges, which forms a maximum spin ordering in these orbitals similar to the case of Hund's rule for atoms (e.g., as in a graphene nanoribbon (GNR) that is a one-dimensional restriction of graphene with edges on both longitudinal sides (Fig. 4a and b) [1–7], in graphene with hexagonal antidot (nanopore) arrays (Fig. 1) [12, 23], and in graphene nanoflakes [13]). This determines the appearance of either ferromagnetism or antiferromagnetism in GNRs [3, 5–7, 12, 13]. Moreover, spin ordering is sensitive to the termination of edge carbon dangling bonds by foreign atoms (e.g., hydrogen (H) and oxygen) and those numbers, which result in the formation of edge  $\pi$  and  $\sigma$  orbitals [3, 8, 25].

Lieb's theorem also predicts the emergence of ferromagnetism by that an increase in the difference between the number of removed A and B sites of the graphene bipartite lattice at zigzag edges induces net magnetic moments (e.g., in nanosize graphene flakes [13] and nanopores [23, 25]).

Few studies, however, have experimentally reported observation of spin related phenomena to arise from zigzag edges in graphenes, although experiments to observe and control graphene edge structures have been conducted using some approaches (e.g., Joule heating [14], fabrication of GNRs [16–18], and formation of graphene antidot lattices (GADLs; graphene nanomeshes) with antidot (i.e., pore) edges [19, 20]). This is because edge-related phenomena are very sensitive to damage, defects, and disorder introduced during fabrication (e.g., by lithographic methods). Thus, we have developed two non-lithographic fabrication methods for graphene edges; i.e., (i) GNRs derived from unzipping of carbon nanotubes combined with air blow and three step annealing [16] and (ii) GADLs fabricated using nanoporous alumina template (NPAT) [26].

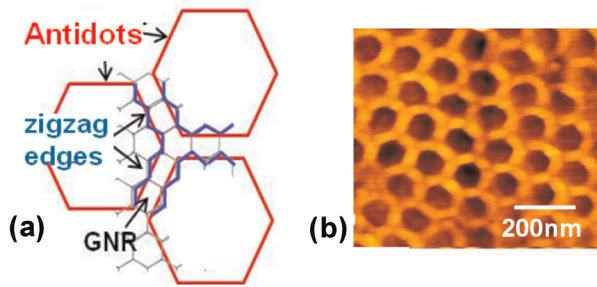


**Figure 1** (online color at: [www.pss-b.com](http://www.pss-b.com)) (a) Schematic view of a GADL. It shows the case that the edge boundaries shown by blue lines are aligned with the carbon hexagonal lattice of graphene to form a zigzag edge. Narrow spaces between two antidots with width ( $W$ ) correspond to GNRs. Actual structure has a larger number of hexagonal carbon unit cells per GNR ( $\sim 40$  nm length and  $W \sim 20$  nm). This GADL structure brings at least three large advantages (Supporting Information (SI 1)). (b) AFM image of a GADL formed by using NPAT as an etching mask, which proves hexagonal shape of antidots with mean diameter  $\phi \sim 80$  nm and mean  $W \sim 20$  nm.

In our previous study [26], low-defect GADLs with honeycomb-like arrays of hexagonal antidots (Fig. 1) were fabricated on a large ensemble of mechanically exfoliated graphenes by using a non-lithographic method (i.e., using NPAT [27] as an etching mask, followed by careful Ar-gas etching) and high-temperature ( $800^\circ\text{C}$ ) annealing in high vacuum and  $\text{H}_2$  atmosphere (see the Supporting Information, online at [www.pss-b.com](http://www.pss-b.com), (SI 1)–(SI 5)). This method at least gave three significant advantages (Supporting Information (SI 1)).

Although we didn't intentionally align the antidot-edge atomic structures to zigzag type unlike Ref. [19], we indirectly confirmed possible presence of zigzag atomic structure at the antidot edges by observation of the small ratios of  $D/G$  peak heights ( $< 0.2$ ) in Raman spectroscopy, which were realized by the high-temperature annealing, by comparing with previous reports [19, 24]. Indeed, presence of polarized spins in such H-terminated GADLs was

confirmed in inter-antidot regions and also at some antidot edges by observation of magnetic force microscope (MFM). Moreover, it was found that the H-terminated zigzag-type GADLs with  $\sim 10$  layers yielded anomalous magnetoresistance (MR) oscillation, which originate from presence of localized electrons at the antidot edges [26].

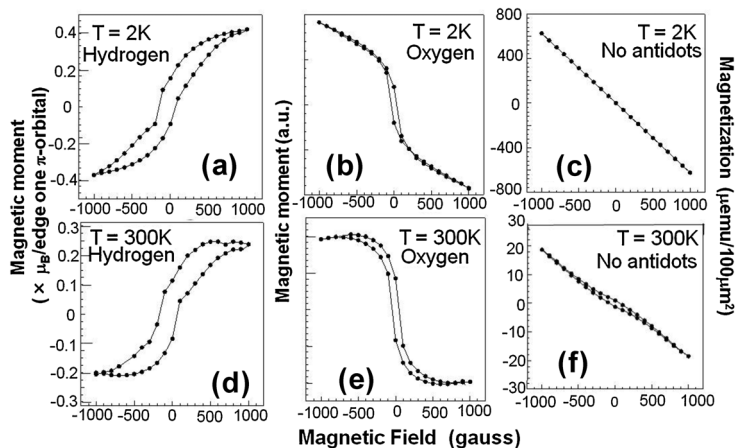
## 2 Experimental results and discussion

### 2.1 Spontaneous spin polarization and ferromagnetism arising from antidot edges

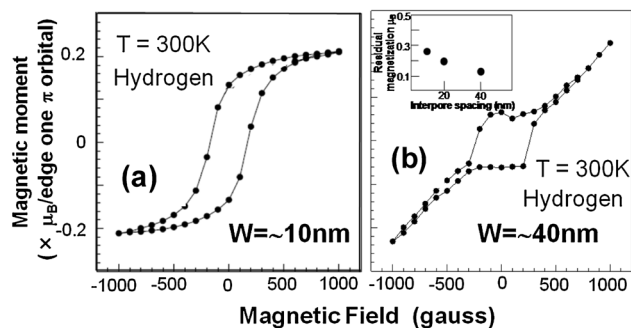
Figure 1a shows a schematic view of a GADL. Atomic force microscopy (AFM) images of a mono-layer GADL formed by using (Fig. 1a) as an etching mask and following our previous method [26] are presented in Fig. 1b. It proves provides a clear evidence of the hexagonal shape of the antidots (Supporting Information, (SI 2)–(SI 4)).

Figure 2a shows a magnetization curve for the H-terminated monolayer of GADL with showing the low  $D/G$  peak ratio values at 2 K (Supporting Information (SI 5)). A ferromagnetic-hysteresis loop with large amplitude is clearly observed. In contrast, this feature becomes a diamagnetism-like weak hysteresis loop for oxygen-terminated GADLs (Fig. 2b; Supporting Information (SI 7)). Bulk graphenes without antidots and those assembled with NPATs show mostly no such features even after  $\text{H}_2$  annealing (Fig. 2c and f; Supporting Information (SI 8)), implying that no parasitic factors (e.g., defects, impurities) of bulk graphenes contribute to the ferromagnetism. It is also confirmed that the features observed at 2 K appear even at room temperature with a larger magnitude of the hysteresis loops (Fig. 2d–f), although the amplitude of magnetization decreases.

In addition to Fig. 2a and d-sample, other three samples with showing the low  $D/G$  peak heights in Raman spectroscopy exhibited similar ferromagnetism. Moreover, no damages or impurities is reconfirmed in the most of bulk-graphene regions, because mechanically exfoliated bulk graphenes show an extremely low  $D/G$  peak heights ( $\ll 0.1$ ) and a high 2D peak intensity in the Raman spectroscopy. This is consistent with the absent ferromagnetism in Fig. 2c and d as mentioned above. These results strongly suggest that



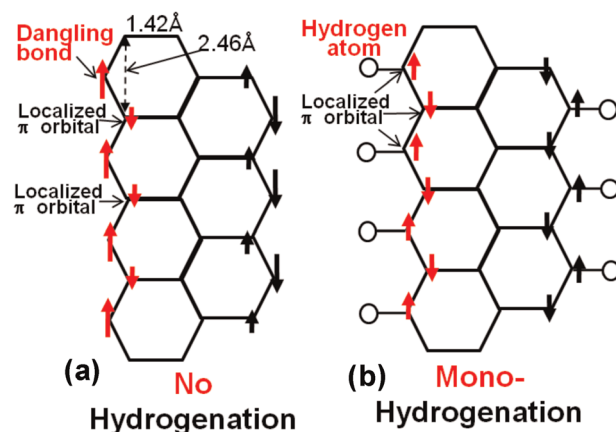
**Figure 2** Magnetization of monolayer GADLs (Supporting Information (SI 5)) with  $\phi \sim 80$  nm and  $W \sim 20$  nm for (a,d) hydrogen-terminated edges; (b,e) oxygen-terminated edges; and (c,f) bulk graphene without antidot arrays. DC magnetization was measured by a superconducting quantum interference device (SQUID; Quantum Design) at 2 K and at room temperature for panels (a)–(c) and panels (d)–(f), respectively. Magnetic fields were applied perpendicular to GADLs. The vertical axes in panels (a) and (d) denote magnetic moment per localized-edge  $\pi$  orbital, assuming mono-hydrogenation of individual edge carbon atoms (Fig. 4b). For Fig. 2d, difference in magnetic moment between upper and lower curves of hysteresis loop at  $H = 0$  (residual magnetization  $B_r \times 2$ ) is  $\sim 0.2 \mu_B$  and the loop width at zero magnetic moment (coercivity  $H_c \times 2$ ) is  $\sim 260$  gauss.



**Figure 3** Correlation of the magnetization with the mean inter-antidot spacing  $W$  of monolayer GADLs.  $W$  corresponds to the mean width of GNRs (Fig. 1a). Mean antidot diameter ( $\phi \sim 80$  nm) was kept through all samples. Values of (residual magnetization  $B_r \times 2$ ) and (coercivity  $H_c \times 2$ ) for Fig. 3a and b are  $\sim 0.28 \mu_B$  and  $\sim 400$  gauss, and  $\sim 0.12 \mu_B$  and  $\sim 500$  gauss, respectively. Inset of (b), Residual magnetization at 300 K as a function of  $W$ , determined from Figs. 2d and 3.

the observed ferromagnetism (Fig. 2a and d) is associated with polarized spins localizing at the H-terminated zigzag-antidot edges.

To reconfirm the contribution of ADL structures to the observed ferromagnetism, the correlation between the inter-antidot spacing (corresponding to the width of the GNR,  $W$ ; Fig. 1a) and the magnetization was measured as shown in Fig. 3. We find that the magnitude of the residual magnetization is inversely proportional to  $W$  value (inset of Fig. 3b). This result is qualitatively consistent with theories



for GNR model according to which the edge spin stability and ordering of a zigzag-edge GNR are determined by the exchange interaction between the two edges leading to vanishing of ferromagnetic edge spin ordering with increase of  $W$  [2, 5].

Such behavior cannot be attributed to the ferromagnetism originating from the defects located only at antidot edges or in the bulk graphene between antidots. Indeed, in the former case ferromagnetism would be mostly independent of  $W$ , while in the latter case ferromagnetism amplitude would increase with an increase of  $W$ . Consequently, we conclude that the observed ferromagnetism is not of parasitic origins (e.g., defects, impurities [28]) but should be purely attributed to H-terminated zigzag antidot edges. This is also consistent with our previous MFM observation [26].

To date, approximately 50% of the samples (5 of the 11 samples measured, which include samples showing the low  $D/G$  peak heights) have shown ferromagnetism (Supporting Information (SI 5)).

As mentioned above, we didn't intentionally align antidot-edge atomic structures to form zigzag. References [14, 15], however, suggested that zigzag edge is the most stable chemically and that arm chair-based edges are stable chemically and that arm chair-based edges are reconstructed to zigzag after electron beam (EB) irradiation for antidot edges and STM Joule heating for long edges of overlapped graphenes (Supporting Information (SI 9) and (SI 10)). This stability may be simply understood by difference in the number of carbon atoms bonded to two neighboring carbon atoms (dangling bonds) for zigzag edge (i.e., one such atom) and arm chair edges (two such atoms) [15]. After removal of

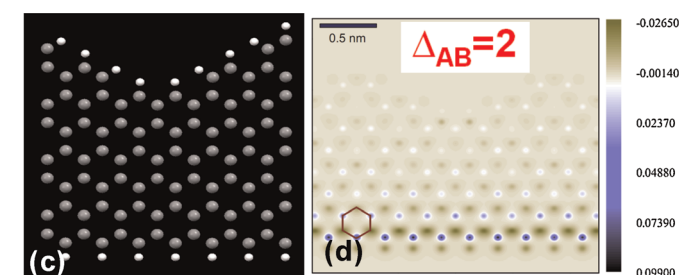


**Figure 4** (online color at: www.pss-b.com) Spin configuration of pure zigzag-edge GNR models (a) without and (b) with mono-H termination. Arrows denote spin moments. Actual structure has a larger number of columns of carbon hexagonal unit cells. For (a), only the dangling bond states contribute to the total magnetic moment with a large exchange splitting. The spin interaction between two zigzag edges yields and stabilizes the antiferromagnetic edge spin ordering by maximizing exchange energy gain, resulting in zero total-magnetism. Neglecting this spin configuration and just counting number of the edge dangling bonds including in the GADL, the magnetic moment per edge dangling bond is estimated to be  $\sim 1.3 \mu_B$ . For (b), edge dangling bonds are mono-hydrogenated (open symbols), resulting in localized edge  $\pi$ -orbital states. Based on (a), the edge magnetic moment can be estimated as  $(\sim 1.3 - 1 \mu_B) = \sim 0.3 \mu_B$ . (c,d) Model and calculation result for Lieb's theorem. (c) Structure of hydrogen passivated quasi-GNR, which employs slight disorder with  $\Delta_{AB} = 2$  (the difference between the number of removed A and B sites of the graphene sublattices at zigzag edges), used for first-principles calculations based on Lieb's theorem. The dark and white atoms are carbon and hydrogen, respectively. (d) Calculated spin-density distribution of quasi-GNR for (c). It gives the edge magnetic moment of  $0.22 \mu_B$ .

such atoms, arm chair edge requires energy two-times larger than zigzag in order to repair the removed atoms and, thus, becomes unstable. In our system, high-temperature annealing for narrow ( $\sim 20$  nm) GNRs might give the energy similar to EB irradiation and Joule heating.

In order to estimate the magnetic moment of edge carbon atoms which contributes to ferromagnetism (Fig. 2), we employ the GNR model assuming zigzag antidot edges at all regions. Assuming that only edge dangling bonds have localized spin moments, the magnetic moment per edge dangling bond prior to H termination (Fig. 4a) is estimated according to the following steps: (1) The total area of assembled bulk graphenes used for the antidot array formation is  $\sim 4$  cm<sup>2</sup>. (2) The area of one hexagonal unit cell with a pore is  $S = 6(3^{-1/2}/2)(a/2)^2 \sim 4300$  nm<sup>2</sup>, where  $a = [80$  nm (antidot diameter) + 20 nm (antidot spacing)]. (3) Thus, the total number of antidots is  $(4$  cm<sup>2</sup>)/(4300 nm<sup>2</sup>)  $\sim 10^{11}$  [(1)/(2)]. (4) The total number of dangling bonds per hexagonal antidot is  $(40$  nm)/(0.142 nm  $\times 3^{1/2}$ )  $\times 6 = 166 \times 6 \sim 1000$ . (5) The total number of edge dangling bonds of the GADL used for the SQUID measurement is  $10^{14}$  [(3)  $\times$  (4)]. Therefore, using (5), the saturation magnetization per edge dangling bond is estimated to be  $1.2 \times 10^{-6}$  (emu)  $\times 10^{-3}/10^{14} = 1.2 \times 10^{-23}$  (J/T). Thus, the magnetic moment per edge dangling bond is, therefore, estimated to be  $(1.2 \times 10^{-23})/(\mu_B = 9.3 \times 10^{-24}) \sim 1.3 \mu_B$ , where  $\mu_B$  is the Bohr magneton. Next, after H annealing at high temperature, edge dangling bonds of a GNR are terminated by H atoms [3, 5–8] (Supporting Information (SI 6) and (SI 12)). Basically, three terminations should be considered: (i) mono-H termination for both edges (Fig. 4b), (ii) di-H termination for both edges, and (iii) mono-H termination for one edge and di-H termination for the other edge.

The type of edge H-termination could not be confirmed in the present experiment. However, we argue that our case corresponds to case (i) from the following reason. The mono-H termination of the edge dangling bond decreases its magnetic moment to one  $\mu_B$ . The magnetic moment of one localized-edge  $\pi$  orbital is, therefore, estimated to be as large as  $(\sim 1.3 - 1 \mu_B) = \sim 0.3 \mu_B$ . This is in fairly good agreement with the theoretical contribution of the  $\pi$ -orbital state to the edge magnetic moment of  $\sim 0.3 \mu_B$  in a zigzag-edged GNR within the ferromagnetically ordered spin configuration [5]. The observed ferromagnetism is stable at least for 1 week even under air atmosphere at room temperature. Why mono-H termination for both edges of a GNR (i.e., edges of the hexagonal antidots) is such stable should be clarified in future.

We have estimated the edge magnetization based on a GNR model with zigzag edges, assuming presence of pure zigzag-antidot edges at all parts of our GADLs. One can admit, however, that a small defect may still present in actual antidot edges. In order to elucidate the influence of such residual small-volume disorder on magnetism of GADL, we performed systematic first-principles calculations of electronic and magnetic properties of quasi-GNR structures

(Fig. 4c) based on Lieb's theorem [23], which assumes the slightly curved upper edge (i.e., disorder). Interestingly, the ground state of quasi-GNR structure turned out to be ferromagnetic in Fig. 4d. The calculated net magnetic moment follows Lieb's theorem with local moments up to  $0.22 \mu_B$  per edge atom and they depend on magnitude of the assumed edge curvature. These values agree fairly well with the value estimated from the GNR model. In order to determine which models (Fig. 4b and c) are more relevant to the actual structures, observation of antidot edge atomic structures is indispensable (Supporting Information (SI 9)).

## 2.2 Hysteresis loop and spin pumping effect in ferromagnetic few-layer GADLs with larger $W$

As mentioned in introduction, we found periodic MR oscillations arising from electrons localizing at H-terminated antidot edges in GADLs with  $\sim 10$  layers [26]. Although we have reported spin polarization at antidot edges of monolayer GADLs in the present study, the GADLs don't show clear electronic features. This might be due to edge contamination and damage originating from formation of electrodes on the GADLs by using lithography. Thus, we measured MR behaviors of H-terminated GADLs with  $\sim 5$  layers, which are thinner than previous GADLs with  $\sim 10$  layers, here. The results are shown in Fig. 5. Although magnitude of spin polarization at antidot edges becomes weaker in the  $\sim 5$  layer GADLs, polarized edge spins should still exist following a theory [22] as well as those in  $\sim 10$  layer GADLs [26]. Indeed, the GADL exhibited small-magnitude ferromagnetism.

Figure 5b and c show MR behaviors measured for inset of Fig. 5a-pattern under a constant current mode of a four probe measurement, when magnetic fields are applied perpendicular to the GADL ( $B_{\perp}$ ) and in parallel with the GADL ( $B_{\parallel}$ ), respectively. In Fig. 5b for perpendicular fields, a weak hysteresis loop is observed. Although it is not clear and MR does not increase (or decrease) with increasing (or decreasing) applied fields, such a hysteresis loop of ferromagnetic materials (e.g., magnetic semiconductors; (InMn)As) conventionally suggests possibility of correlation with the observed ferromagnetic magnetization loop (Fig. 2a and d) and polarized spins at the antidot edges.

In the present case, spin-polarized electrons localize at the antidot edges under thermal equilibrium. However, under non-thermal equilibrium with a constant current flow for Fig. 5a, the flat bands at the antidot edges weaken and, thus, polarized edge-electron-spins can flow between electrodes somehow. Moreover, Fig. 5a-sample has larger  $W$  value. Hence, localization of the edge-polarized spins become weaker (Fig. 3b) and the polarized spins can become to transverse via. large inter-antidot regions. Nevertheless, the amount of polarized spin flow might be not enough for appearance of a conventional ferromagnetic MR hysteresis loop, because the measured GADL is not monolayer but  $\sim 5$  layers. Moreover, scattering of electrons by the honeycomb-like antidot array under magnetic fields [26] obstruct the spin flow and emergence of a conventional hysteresis loop. It

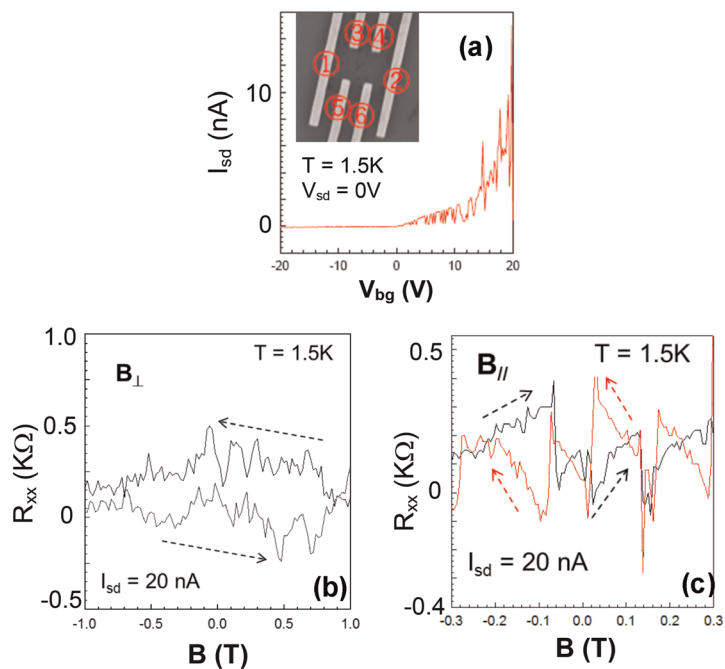


**Figure 5** (online color at: [www.pss-b.com](http://www.pss-b.com)) MR behaviors of a ferromagnetic  $\sim 5$ -layer GADL with  $W \sim 30$  nm. (a) Current flow between electrodes 1 and 2 (see inset) as a function of back gate voltage ( $V_{bg}$ ) at a constant voltage of 0 V. It exhibits an n-type semiconductive behavior due to the GNR structure (Fig. 1a). Inset, SEM image of electrode pattern formed on a GADL with  $\sim 5$  layers for MR measurements. MR ( $R_{xx}$ ) between electrodes 5 and 6 was measured under a constant current flow of 20 nA between electrodes 1 and 2. (b,c) MR ( $R_{xx}$ ) behaviors under perpendicular (b) and parallel (c) fields.  $V_{bg}$  was set to +20 V shown in Fig. 5a for both measurements. Arrows mean sequence of applied  $B$  (e.g., from  $-1$  T to  $+1$  T or from  $+1$  T to  $-1$  T). Weak-magnitude hysteresis loop for (b) and saw-tooth like oscillations for (c) are observed. Such features have not been observed in GADLs with  $W \sim 20$  nm.

provides a chance to realize all-carbon spin transistors like magnetic semiconductors.

On the other hand, Fig. 5c for parallel fields shows anomalous saw-tooth like oscillations, in which MR monotonically increases with increasing fields, while it abruptly decreases at a field and starts to increase again in a repeated manner. We call this process as spin pumping effect. The effect means a repeated cycle of accumulation of polarized spins and its abrupt emission, depending on applied magnetic fields. Such anomalous behaviors cannot be interpreted by any previous MR phenomena (e.g., ferromagnetic behavior, giant MR, tunnel MR, and spin valve).

The effect might be qualitatively understood as follows. When applied parallel magnetic field increases, free polarized spins appear in large  $W$  spaces and accumulate at the flat energy band at the antidot edges in addition to the edge-localized spins. However, the accumulation of edge spins saturate and the excess spins are abruptly emitted at a critical field, as parallel magnetic fields increase further, because the flat band is modulated by the parallel fields. After the emission of the accumulated spins, the antidot edges can allow accumulation of further spins and the flat band also recovers near to the initial condition somehow. Then, MR starts to increase again. These are MR behaviors unique to the present GADLs with field applied in parallel.

**3 Conclusions** In conclusion, we successfully fabricated low-defected mono-layer GADLs by using a non-lithographic method (i.e., using NPAT) and evidenced the emergence of spontaneous spin polarization (large-amplitude ferromagnetism) when the GADLs were hydrogen-terminated. It could be attributed to the zigzag pore-edges in

agreement with our GNR and quasi-GNR models (Lieb's theorem). Moreover, a MR loop and spin pumping effect were found for perpendicular and parallel fields in ferromagnetic few-layer GADLs with larger  $W$ . In a view of recent theoretical reports on spin-filtering effect [21] and (quantum) spin Hall effect (QSHE) [29–33] using edge spin current of graphene, our observations pave a way toward creation of novel spintronic devices. Furthermore, the present all-carbon and mono-atomic layer ferromagnetism must realize rare-element free and ultra-light magnets, which overcome energy-resource threats.

**Acknowledgements** The authors thank K. Fujita, Y. Hashimoto, E. Endo, S. Katsumoto, Y. Iye, M. Yamamoto, S. Tarucha, T. Enoki, M. Koshino, T. Ando, T. Muranaka, J. Akimitsu, T. Yamaoka, N. Nagaosa, H. Aoki, S. Roche, P. Kim, X. Jia, and M. S. Dresselhaus for their technical contribution, fruitful discussions, and encouragement. This work at Aoyama Gakuin was partly supported by a Grant-in-aid for Scientific Research and a High-Technology Research Center Project for private universities in MEXT, and also AFOSR grant. M. C. and H. X. Y. acknowledge support by French ANR PNANO project “Nanosim-Graphene” and Grenoble Nanosciences Foundation.

## References

- [1] K. Nakada, M. Fujita, G. Dresselhaus, and M. S. Dresselhaus, *Phys. Rev. B* **54**, 17954 (1996).
- [2] M. Fujita et al., *J. Phys. Soc. Jpn.* **65**, 1920 (1996).
- [3] K. Kusakabe and M. Maruyama, *Phys. Rev. B* **67**, 092406 (2003).
- [4] S. Okada and A. Oshiyama, *Phys. Rev. Lett.* **87**, 146803 (2001).
- [5] H. Lee et al., *Phys. Rev. B* **72**, 174431 (2005).
- [6] R. G. A. Veiga et al., *J. Chem. Phys.* **128**, 201101 (2008).

- [7] H. Lee et al., Chem. Phys. Lett. **398**, 207 (2004).  
 [8] T. Enoki et al., Solid State Commun. **149**, 1144–1150 (2009).  
 [9] Y. Niimi et al., Phys. Rev. B **73**, 085421 (2006).  
 [10] Y.-W. Son et al., Phys. Rev. Lett. **97**, 216803 (2006).  
 [11] L. Yang, S. G. Louie, et al., Phys. Rev. Lett. **99**, 186801 (2007).  
 [12] N. Shima et al., Phys. Rev. Lett. **71**, 4389 (1993).  
 [13] J. F. Rosser and J. J. Palacios, Phys. Rev. Lett. **99**, 177204 (2007).  
 [14] X. Jia, M. S. Dresselhaus, et al., Science **323**, 1701 (2009).  
 [15] C. O. Girit et al., Science **323**, 1705 (2009).  
 [16] T. Shimizu, J. Haruyama, et al., Nature Nanotechnol. **6**, 45 (2011).  
 [17] M. Y. Han et al., Phys. Rev. Lett. **104**, 056801 (2010).  
 [18] X. Wang et al., Phys. Rev. Lett. **100**, 206803 (2008).  
 [19] B. Krauss et al., Nano Lett. **10**, 4544 (2010).  
 [20] J. Bai et al., Nature Nanotechnol. **5**, 190 (2010).  
 [21] Y.-W. Son et al., Nature **444**, 347 (2006).  
 [22] M. Otani et al., Phys. Rev. B **81**, 161403 (R) (2010).  
 [23] H. Yang et al., <http://arxiv.org/abs/1103.4188>.  
 [24] Y. You et al., Appl. Phys. Lett. **93**, 163112 (2008).  
 [25] D. Soriano et al., Phys. Rev. Lett. **107**, 016602 (2011).  
 [26] T. Shimizu, J. Nakamura, K. Tada, Y. Yagi, and J. Haruyama, Appl. Phys. Lett. **100**, 023104 (2012).  
 [27] I. Takesue, J. Haruyama, et al., Phys. Rev. Lett. **96**, 057001 (2006).  
 [28] H. Asano, S. Muraki, H. Endo, and S. Iijima, J. Phys.: Condens. Matter **22**, 334209 (2010).  
 [29] S. Murakami et al., Science **301**, 1348 (2003).  
 [30] C. L. Kane and E. J. Mele, Phys. Rev. Lett. **95**, 226801 (2005).  
 [31] C. L. Kane, J. Modern Phys. B **21**, 1155 (2007).  
 [32] M. J. Schmidt and D. Loss, Phys. Rev. B **81**, 16 5439 (2010).  
 [33] D. A. Abanin, A. K. Geim, et al., Science **332**, 328 (2011).